

**AERODYNAMIC OPTIMIZATION OF MEDIUM
ALTITUDE LONG ENDURANCE UNMANNED
AERIAL VEHICLE**

MUHAMMAD REZZA BIN RITZWAN

**SCHOOL OF AEROSPACE ENGINEERING
UNIVERSITI SAINS MALAYSIA
2021**

ENDORSEMENT

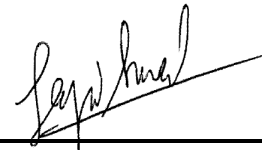
I, Muhammad Rezza Bin Ritzwan hereby declare that I have checked and revised the whole draft of dissertation as required by my supervisor.



(Signature of Student)

Name: Muhammad Rezza Bin Ritzwan

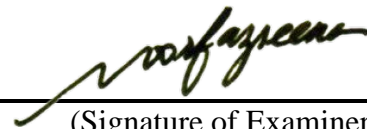
Date: 9 July 2021



(Signature of Supervisor)

Name: Prof Madya Dr. Farzad Ismail

Date: 10 July 2021



(Signature of Examiner)

Name: Dr Noorfazreena M. Kamaruddin

Date: 9 July 2021

DECLARATION

This thesis is the result of my own investigation, except where otherwise stated and has not previously been accepted in substance for any degree and is not being concurrently submitted in candidature for any other degree.



(Signature of Student)

Name: Muhammad Rezsa Bin Ritzwan

Date: 9 July 2021

ACKNOWLEDGEMENT

The completion and success of this thesis required a lot of guidance and support from numerous people. First and foremost, I would like to offer my highest gratitude to my supervisor, Assoc. Prof. Dr Farzad Ismail for believing in me and for allowing me to work with him. Prof Madya Dr Farzad Ismail has been my source of knowledge and advice throughout this project. With his support, I managed to learn about everything required in doing this project.

Besides, I would like to thank you to all the lecturer, especially Dr Chang Wei Shyang, to conduct the weekly meeting on the Microsoft team. I also would love to express my gratitude to the staff and technicians because they were there whenever I need help. Furthermore, I could not go any further without acknowledging the tremendous contributions of my PhD friends Safie who helped me a lot during my journey to finish this project. I also was supported by many people and friends; hence I would again express my gratitude to those who lend their helping hands when I was in difficulty. Finally, I would like to express my appreciation to my family and my parents, who have supported me unconditionally since the beginning of my studies at USM. You have helped me like no other person in my hour of need, and you have taught me essential values that should be the essence of every researcher and educator. Therefore, I dedicate this thesis to you.

Thank you all.

ABSTRAK

Matlamat penyelidikan ini adalah untuk mengoptimumkan sayap utama Kenderaan Udara Tanpa Pemandu (UAV) menggunakan teori aerodinamik subsonik rendah dan analisis CFD. Lang Merah UAV adalah UAV semasa yang dikendalikan oleh USM. Tesis ini bermaksud menghasilkan peningkatan prestasi sekurang-kurangnya 10% berbanding sayap Lang Merah dengan memasukkan sayap yang diperbaiki. Kerana peningkatan permintaan baru-baru ini untuk Kenderaan Udara Tanpa Pemandu dalam industri aeroangkasa, mengoptimumkan prestasi platform ini sangat penting. Perisian berbantuan komputer (CAD) perisian SOLIDWORKS CAD 2021 dan ANSYS WORKBENCH digunakan untuk menjalankan analisis simulasi. Pengesahan hasil simulasi adalah mustahak untuk membandingkan hasilnya. Penemuan simulasi disahkan menggunakan data NACA 4412. Penyediaan simulasi projek ini berdasarkan persediaan eksperimen Universiti Baylor. Konfigurasi yang digunakan oleh Baylor University untuk mendapatkan hasil eksperimen NACA 4412 mempunyai bilangan Reynolds 150 000, lebar sayap 24 inci, dan kord 6 inci. Ujian bebas grid (GIT) dilakukan untuk menurunkan kos pengiraan dan jangka masa simulasi Hasilnya menunjukkan bahawa peningkatan prestasi mencapai pengoptimuman aerodinamik sayap yang diperlukan. Penemuan simulasi mendedahkan peningkatan 9% L/D untuk sayap 3D pada sudut luncuran 2 darjah dan kenaikan 10.8% dalam $C_L^{3/2}/C_D$ untuk sayap 3D pada sudut yang sama.

Kata Kunci: Kenderaan Udara Tanpa Pemandu, Dinamik Cecair Komputasi, Sayap, Hujung Sayap, Airfoil

ABSTRACT

The goal of this research is to optimize the primary wing of a MALE UAV using low subsonic aerodynamic theories and CFD analysis. Lang Merah UAV is the current UAV operated by USM. This thesis intends to produce a performance boost of at least 10% over the Lang Merah wing by incorporating an improved wing. Because of the recent increase in demand for MALE UAVs in the aerospace industry, optimizing the performance of these platforms is critical. Computer-aided design (CAD) software SOLIDWORKS CAD 2021 Edition and ANSYS WORKBENCH are used to conduct the simulation analysis. Validation of the simulation result is essential in order to compare the results. The simulation findings were validated using NACA 4412 data. This project simulation's setup is based on the Baylor University experimental setup. The configuration employed by Baylor University to obtain the experimental result of the NACA 4412 has a Reynolds number of 150 000, a wingspan of 24 inches, and a chord length of 6 inches. A grid independent test (GIT) is performed in order to lower the simulation's computational cost and run duration. The results show that improving performance achieves the required wing aerodynamic optimization. The simulation findings reveal a 9% increase in L/D for a 3D wing at a gliding angle of 2 degrees and a 10.8% rise in $C_L^{3/2}/C_D$ for the 3D wing at the same angle.

Keywords: Unmanned Aerial Vehicle, Computational Fluid Dynamic, Wing, Wingtip, Airfoil

TABLE OF CONTENTS

ENDORSEMENT	I
DECLARATION.....	II
ACKNOWLEDGEMENT.....	III
ABSTRAK	IV
ABSTRACT.....	V
TABLE OF CONTENTS	VI
LIST OF TABLES	IX
LIST OF FIGURES	X
LIST OF SYMBOLS	XIII
LIST OF ABBREVIATIONS	XV
CHAPTER 1 INTRODUCTION	16
1.1 Overview	16
1.2 Research Background.....	16
1.3 Problem Statement	19
1.4 Objectives.....	20
1.5 Scope of Work.....	20
1.6 Thesis Outline	21
CHAPTER 2 LITERATURE REVIEW	23
2.1 Low Reynolds Number Aerodynamic.....	23
2.2 Flow Separation.....	26
2.3 Aerodynamic Force	29
2.4 Glide Ratio	30
2.5 Aerodynamic Drag	32
2.5.1 Parasite Drag	
2.5.2 Lift-Induced Drag	

2.6	Coefficient of Drag and Coefficient of Lift	35
2.7	Airfoils in General.....	37
2.7.1	Nomenclature of An Airfoil	
2.7.2	Effects of Airfoils Geometry	
2.8	Angle of Attack (AoA).....	43
2.9	Computational Fluid Dynamic (CFD).....	46
2.9.1	Definition of Mesh vs Grid	
2.9.2	Meshing Generalities	
2.9.3	Mesh Topology (Single Block)	
CHAPTER 3	METHODOLOGY	53
3.1	Overview	53
3.2	Design Research.....	54
3.3	2D Airfoil Model CAD Design.....	56
3.3.1	2D Airfoil Design Parameter.....	57
3.4	2D Aerodynamic Analysis	59
3.5	2D Meshing Grid Independent Test	59
3.6	2D Meshing Set up.....	62
3.6.1	2D Airfoil Fluid Domain Geometry Setup	
3.7	2D Solver Setup	67
3.8	3D Airfoil & Wing Model CAD Design.....	68
3.8.1	3D Airfoil & Wing Design Parameter.....	71
3.9	3D Aerodynamic Analysis	74
3.10	3D Airfoil and Wing Meshing Set Up	74
3.10.1	3D Airfoil & Wing Fluid Domain Setup.....	84
3.11	3D Solver Set Up.....	85
CHAPTER 4	RESULT AND DISCUSSION	87
4.1	Baylor University Experiment Results.....	87

4.2	RANS Model Results Comparison	91
4.2.1	C_l VS AoA.....	91
4.2.2	C_d VS AoA	92
4.2.3	L/D VS AoA.....	94
4.2.4	Flow Over Airfoil.....	95
4.2.5	GIT Comparison Between K-Epsilon & Spalart Allmaras	98
4.3	Simulation Validation	100
4.4	2D Airfoil Simulation Results.....	103
4.4.1	C_l VS AoA.....	103
4.4.2	C_d VS AoA	106
4.4.3	L/D VS AoA.....	107
4.4.4	Drag Curve	110
4.5	2D Airfoil to 3D Wing Calculation and Results	110
4.6	3D Wing Simulation Results.....	122
4.6.1	Effect of Vortex Towards Aerodynamic Performance.....	123
CHAPTER 5 CONCLUSION AND FUTURE RECOMMENDATIONS ...		127
5.1	Conclusion.....	127
5.2	Recommendations for Future Research	128
REFERENCES		
APPENDIX A: 2D & 3D Meshing Setup		
APPENDIX B: 2D AIRFOIL SOLVER SETUP		
APPENDIX C: Lang merah (lm2-20) review		

LIST OF TABLES

	Page
Table 1.1 Various UAV applications.....	17
Table 3.1 Basic design parameter of 2D airfoil	58
Table 3.2 2D Fluent GIT result.....	62
Table 3.3 Mesh quality of 2D fluid domain (4412).....	65
Table 3.4 Mesh quality of 2D fluid domain (Lang Merah)	65
Table 3.5 Mesh quality of 2D fluid domain (S1091).....	65
Table 3.6 Skewness range and cell quality	67
Table 3.7 Average value wall Y^+ for all the airfoil.....	68
Table 3.8 Basic design parameter of 3D airfoil	72
Table 3.9 Average Mesh quality of 3D fluid domain	83
Table 4.1 Data from the Baylor University experiment	90
Table 4.2 The C_l value for all the turbulence model.....	91
Table 4.3 The C_d value for all the turbulence model	92
Table 4.4 The L/D value for all the turbulence models	94
Table 4.5 Lift coefficient data of the GIT for both model.....	98
Table 4.6 Simulation Results for NACA4412 airfoil	101
Table 4.7 Results of C_l vs AoA of the 3 airfoil.....	104
Table 4.8 C_d data for the 3 airfoils.....	106
Table 4.9 L/D data of the 3 airfoils.....	108
Table 4.10 Results for the 3 Wing	119
Table 4.11 L/D ratio value for all the 3 wings.....	120
Table 4.12 Results of 3D model at 2 degrees AoA from the simulation.....	123

LIST OF FIGURES

	Page
Figure 2.1 Effect of Reynolds number on airfoil maximum sectional lift-to-drag ratio	24
Figure 2.2 Illustration highlighting conventional airfoil separation characteristics at different Reynolds number regimes below 10^6	27
Figure 2.3 Forces acting on an aircraft	29
Figure 2.4 Type of aircraft and their glide ratio.....	31
Figure 2.5 Typical drag breakdown	32
Figure 2.6 Laminar vs conventional flow	37
Figure 2.7 Conventional airfoils	38
Figure 2.8 Terminology of an airfoil	39
Figure 2.9 Basic nomenclature of an airfoil.....	40
Figure 2.10 Pressure distributions over symmetric and cambered airfoils	41
Figure 2.11 Effect of camber on an airfoil's lift coefficient	42
Figure 2.12 Streamlines in a steady flow over a cambered airfoil.....	43
Figure 2.13 Angle of attack	44
Figure 2.14 Variation of Angle of attack vs Coefficient of Lift	45
Figure 2.15 Variation in Angle of attack vs Coefficient of Drag	45
Figure 2.16 A meshed domain	49
Figure 2.17 Methodology of general grid generation	51
Figure 2.18 Domain Topology (O-Type, C-Type, and H-Type; from left to right) ..	52
Figure 3.1 Illustration of the flow chart methodology	54
Figure 3.2 Airfoil design with their characteristics	55
Figure 3.3 2D airfoil model on design modeler of ANSYS WORKBENCH.....	57

Figure 3.4 Surface planar of 2D airfoil	58
Figure 3.5 The model (a) flow domain (b) airfoil geometry (c) the meshing (d) mesh refinement at the airfoil surface	61
Figure 3.6 2D FLUENT GIT result	62
Figure 3.7 Mesh set up for 2D airfoil	63
Figure 3.8 Named selection for boundary condition of 2D airfoil	64
Figure 3.9 Rectangular fluid domain for 2D airfoil	64
Figure 3.10 Misalignment of midpoints for skewed grid	66
Figure 3.11 3D airfoil model on design modeler of ANSYS WORKBENCH.....	69
Figure 3.12 (a) & (b) Different view of the 3D airfoil model.....	70
Figure 3.13 3D wing model on design modeler of ANSYS WORKBENCH	70
Figure 3.14 (a) & (b) Different view of 3D wing model design.....	71
Figure 3.15 Domain size of the 3D airfoil	72
Figure 3.16 Domain size of the 3D wing	73
Figure 3.17 Domain that added of the 3D airfoil.....	73
Figure 3.18 Example of a structured grid	75
Figure 3.19 (a) & (b) Domain mesh of 3D airfoil.....	77
Figure 3.20 Detail view of the 3D airfoil mesh	77
Figure 3.21 Wireframe mesh view of the 3D airfoil.....	78
Figure 3.22 (a) & (b) Domain mesh of 3D wing	79
Figure 3.23 Other side of the wall	79
Figure 3.24 Wireframe mesh view of the 3D wing	80
Figure 3.25 3D airfoil inflation layer in the wall boundary layer.....	81
Figure 3.26 Detail view of 3D airfoil inflation layer in the wall boundary layer	81
Figure 3.27 3D airfoil named selection for boundary conditions	83
Figure 3.28 3D wing named selection for boundary conditions.....	83

Figure 3.29 (a) & (b) 3D model fluid domain setup	85
Figure 4.1 Lift coefficient versus AoA from Baylor University experimental data..	88
Figure 4.2 Drag curve from the experimental data	89
Figure 4.3 Polynomial graph of C_d versus C_l from the experiment results.....	90
Figure 4.4 Graph of C_l vs AoA	92
Figure 4.5 Graph of C_d vs AoA	93
Figure 4.6 L/D ratio vs AoA graph.....	95
Figure 4.7 Velocity contours and streamlines of the airfoil at angle of attack of 12° (a) k- ϵ Realizable (b) k- ω SST and (c) Spalart-Allmaras	97
Figure 4.8 Realizable k- ϵ model GIT graph	99
Figure 4.9 Spalart Allmaras model GIT graph	99
Figure 4.10 Graph of C_l against AoA	101
Figure 4.11 Graph of C_d against AoA.....	102
Figure 4.12 Graph of L/D ratio against AoA	102
Figure 4.13 Graph of lift coefficient against angle of attack	104
Figure 4.14 Graph of drag coefficient against angle of attack.....	107
Figure 4.15 L/D ratio against AoA graph	109
Figure 4.16 Drag curve for the 3 airfoils	110
Figure 4.17 C_l vs AoA for NACA 4412 airfoil.....	111
Figure 4.18 C_l vs AoA for Lang Merah airfoil.....	115
Figure 4.19 C_l VS AoA for S1091 airfoil	117
Figure 4.20 Endurance graph for the 3 wing	120
Figure 4.21(a)normal & (b)detail view of vector line flow of 3D airfoil	124
Figure 4.22 (a)Velocity & (b)Pressure distribution of the 3D wing	124
Figure 4.23 Detail view of vector line flow of 3D wing.....	125

LIST OF SYMBOLS

α	Angle of attack
α_g	Geometric angle of attack
$\alpha_{l=0}$	Zero lift angle of attack
b	Span
c	Chord
C_d	Airfoil drag coefficient
C_{d0}	Profile drag coefficient
C_l	Airfoil lift coefficient
C_{lmax}	Maximum lift coefficient
C_D	Drag coefficient
C_{Di}	Induced drag coefficient
C_L	Lift coefficient
D	Drag
e	Oswald's efficiency factor
$k-\epsilon$	K-epsilon
$k-\omega$	K-omega
K	Kelvin
L	Lift
m	Meter
M	Mach number
Re	Reynolds Number
S	Planform area
t/c	Thickness ratio
T	Thrust
V	Velocity

V_{∞}	Free stream velocity
W	Weight
x	Coordinate axis
y	Coordinate axis
z	Coordinate axis
ρ	Atmospheric density
π	pi

LIST OF ABBREVIATIONS

ACTD	Advanced Concept Technology Demonstrator
AoA	Angle of Attack
AR	Aspect Ratio
CAD	Computer Aided Design
CFD	Computational Fluid Dynamic
CPU	Central Processing Unit
DARPA	Defence Advanced Research Project Agency
GIT	Grid Independent Test
GPS	Global Positioning System
HALE	High Altitude Long Endurance
LALE	Low Altitude Long Endurance
LSB	Laminar Separation Bubble
MALE	Medium Altitude Long Endurance
PIV	Particle Image Velocimetry
RANS	Reynolds averaged Navier Stokes
SST	Shear-Stress Transport
UAV	Unmanned Aerial Vehicle
USM	Universiti Sains Malaysia

CHAPTER 1

INTRODUCTION

1.1 Overview

A medium altitude long endurance UAV (MALE UAV) is an unmanned aerial vehicle (UAV) that flies at an altitude window of 10,000 to 30,000 feet (3,000–9,000 m) for extended durations of time, typically 24 to 48 hours (Weibel & Hansman, 2005).

1.2 Research Background

Drones are unmanned aerial vehicles (UAVs). A drone is a flying robot that can fly (Bappy et al., 2015). The flying machine can be controlled remotely or fly autonomously thanks to software-controlled flight plans in their embedded systems, which work in conjunction with GPS. The military is the most common user of drones. Weather monitoring, firefighting, search and rescue, surveillance, traffic monitoring, and other applications are possible (Jung et al., 2019). Drones have gained popularity in recent years due to a variety of business applications. Amazon declared in late 2013 that it would deploy unmanned aerial vehicles for deliveries in the future in the surrounding areas. Amazon Prime Air is a service that promises to deliver orders within 30 minutes within a 10-mile radius (Bappy et al., 2015). As a result, domestic UAV use, rather than military use, has a bright future in various areas.

Table 1.1 Various UAV applications

Remote Sensing
Commercial Aerial Surveillance
Commercial and Motion Picture Film
Domestic policing
Oil, gas and mineral exploration and production
Disaster relief
Scientific research
Armed attacks
Aerial target exercise for training purpose
Search and rescue
Conservation
Maritime patrol
Forest fire detection
Archaeology

Drones for military usage began in the mid-1990s with the Defence Advanced Research Projects Agency (DARPA) and Defence Airborne Reconnaissance Office (DARO High-Altitude)'s Endurance Unmanned Aerial Vehicle Advanced Concept Technology Demonstrator (HAE UAV ACTD) programme (Bappy et al., 2015). This ACTD laid the groundwork for the Global Hawk's upgrade. The Global Hawk can hover at heights of up to 65,000 feet and fly for up to 35 hours at speeds of up to 340 knots. It costs around \$200 million (Sovon, 2017). It has a wingspan of 116 feet and a range of 13,809.4 miles, which is a great distance. Global Hawk was created to address two primary needs, which is homeland security and drug prohibition (Clark, 2009).

The Predator, which was similarly built in the mid-1990s but has since been enhanced with Hellfire missiles, is another highly effective drone. Predator is the most combat-proven Unmanned Aircraft System (UAS) globally, according to Smithsonian's Air & Space magazine, which named it one of the top 10 aircraft that transformed the world. The first Predator, constructed by General Atomics, can fly at 25,000 feet for 40 hours at a top speed of 120 miles per hour (Bappy et al., 2015).

Unmanned aerial vehicles (UAVs) with low-altitude long-endurance (LALE), medium-altitude long-endurance (MALE), and high-altitude long-endurance (HALE) technologies have become increasingly important as a result of various desires, including, in particular, extending internet coverage to remote areas where there is no mobile network coverage. LALE, MALE, and HALE UAVs, in general, fly up to 3000 m, between 3000 and 9000 m, and over 9000 m, respectively, with flight time increasing exponentially as operation altitude increases. HALE UAVs, for example, are designed to fly endlessly without requiring any external energy source other than solar power or a hydrogen-based fuel cell (Jung et al., 2019).

In this study, the primary wing of MALE UAV was chosen for the optimization of aerodynamic behaviour under low subsonic conditions through Computational Fluid Dynamic (CFD) to analyze the lift coefficient (C_L) and drag coefficient (C_D). The airfoil chosen is compared to the Lang Merah airfoil. Through the simulation, a suitable wing design with the highest $C_L^{3/2}/C_D$ will be chosen.

1.3 Problem Statement

Any aircraft that does not have a human pilot onboard is referred to as an unmanned aerial vehicle (UAV). UAVs date back to 1915, when Nikolai Tesla published a dissertation describing "an armed, pilotless aircraft designed to defend the United States" (Roadmap, 2011). UAVs are available in a variety of sizes, designs, and functions. UAVs were originally only remotely piloted; now, autonomous control is becoming more common. As UAV technology improves and costs decrease, they become a fascinating choice for various difficult jobs, particularly when long-range drones are accessible. Medium altitude long endurance unmanned aerial vehicles are in high demand because of their important role (Panagiotou et al., 2018). However, improving the aerodynamics of medium altitude long endurance UAVs has considerable challenges. So, for my final year project I am attempting to learn more about the aerodynamics of the UAV and how to make it operate so that it can assist in this field.

At $10^4 < Re < 10^5$, there is a limitation of data on the forces created by airfoils and wings. Only one study by Laitone, (1997) targeted specifically on this range of Re , and it was also the only one that looked at airfoils and wings at $Re < 5 \times 10^4$. Every other study tended to concentrate on $Re > 10^5$ (McArthur, 2007). Because UAVs are already being manufactured with operational Re as low as 3×10^4 , and there is a lot of interest in operating at even lower Re , it's critical to understand how the forces created change along the whole range of $10^4 < Re < 10^5$ (McArthur, 2007). Thus, this project will be focused on Reynolds number slightly more than 1×10^5 which is 1.5×10^5 .

This project will provide a basis or platform for future development of MALE UAV capability at University Science of Malaysia's School of Aerospace Engineering.

Before this study, there was no well-documented research at USM that focused on aerodynamic analysis and optimization of MALE UAVs, particularly employing CFD methods.

1.4 Objectives

This study will evaluate the aerodynamic flow of the UAV. In addition, the project objective will analyze the effect of aerodynamic behaviour on the various airfoil. Goals that are to be achieved in this project include:

- i. To study the best aerodynamic behavior (L/D) of the various airfoil for a MALE UAV.
- ii. To improve the endurance on the MALE UAV in term of glide ratio ($C_L^{3/2}/C_D$).
- iii. To study the vortex and downwash effect on the lift towards the wing of the MALE UAV.

1.5 Scope of Work

The accurate simulation results for the airfoil and wing are challenging projects that require many processes to be completed. Therefore, the project scope of work for this project are as follow:

- i. To study the wing aerodynamics for MALE UAV at low speed conditions.
- ii. To provide a reasonable wing type for the MALE UAV design as part of assisting the School of Aerospace Engineering drone team at USM.

1.6 Thesis Outline

This thesis is divided into five main chapters, each of which describes the project in depth. The MALE UAV is introduced in the first chapter. It gives an overview of the UAV project's history. Next, this section delves into the UAV's actual design and application. This chapter then defines the problem statement, project goals, and project scope of activity and study.

The second chapter goes through all of the literature and theoretical basis for this research and endeavour. This chapter focuses on the findings and research done by others in a journal linked to the aerodynamic airfoil project produced. The goal of this chapter is to gather information and knowledge related to the project field. This part also covered the theory and fundamentals of aerodynamics that were employed in this project.

The approach and setting used in this project are explained in depth in Chapter 3. This chapter began with an overview of the project's overall flow before delving into the specifics. The technique describes the airfoil configuration, mesh setup, and solver setup.

The findings of the simulation results analysis are presented in Chapter 4, along with a discussion. This chapter discussed the research's findings and conclusions and the explanations for a specific result achieved through simulation and analytical analysis, as well as the methodology's justifications. This chapter discusses the comparison of simulation and experimental data to arrive at a valid conclusion. The findings are then compared to the wing performance of Lang Merah.

This research and the project's conclusion and recommendations are included in Chapter 5. Next, the overall project's comprehensive overview, which summarises the project's development process, is completed. Finally, some recommendations and further work for the future development of this MALE UAV project are given at the conclusion of this thesis.

CHAPTER 2

LITERATURE REVIEW

2.1 Low Reynolds Number Aerodynamic

Researchers like Schmitz, (1967) studied the impact and performance of the airfoil by lowering the Reynolds as early as 1930. Within a Reynolds number range of 2×10^4 to 2×10^5 , Schmitz tested three airfoils: a thin flat plate, a thin cambered plate, and a standard N60 airfoil (12.4% t/c, 4% camber). Two significant findings emerged from Schmitz research are thin plate airfoils regularly outperformed thick plate airfoils below $Re 10^5$, and flow separation is more likely below $Re 10^5$, particularly for the thicker N60. Researchers like Mueller, Selig, and Hoerner revived interest in low-Re aerodynamics in the 1980s, and their investigations corroborated Schmitz's findings. Below the Reynolds number of 10^5 , thin flat and cambered plates are more efficient compared to the conventional airfoils. Another result was that the cambered plates exhibit minor changes in the lift coefficient (C_l) and drag coefficient (C_d) as the Reynolds number increases.

In contrast, flat plates stay essentially constant, as shown in Figure 2.1. Hoerner demonstrated that the maximum lift coefficient (C_{lmax}) of the cambered plate increased by 4% between Reynolds numbers of 4×10^4 and 1.2×10^5 , whereas that of the N60 airfoil increased by almost 180% (Hoerner, 1965). (Selig et al., 1989) and (Mueller & Batill, 1982) conducted low-Reynolds-number experiments on a variety of airfoils and found that the C_{lmax} is consistently increasing with higher Reynolds numbers and that the minimum drag coefficient is significantly decreasing above a Reynolds number of 10^5 . Selig also noted that the drag polar was discernibly comparable for the 60 sailplane-type airfoils examined and was virtually indifferent to Reynolds number

changes once above 10^5 . However, there was a lot of non-linearity in the drag polar below this threshold (Selig et al., 1989). The first findings from every single of these experiments showed that low Reynolds number airfoil performance was significantly dependent on the airfoil's shape and the Reynolds number at which it operated.

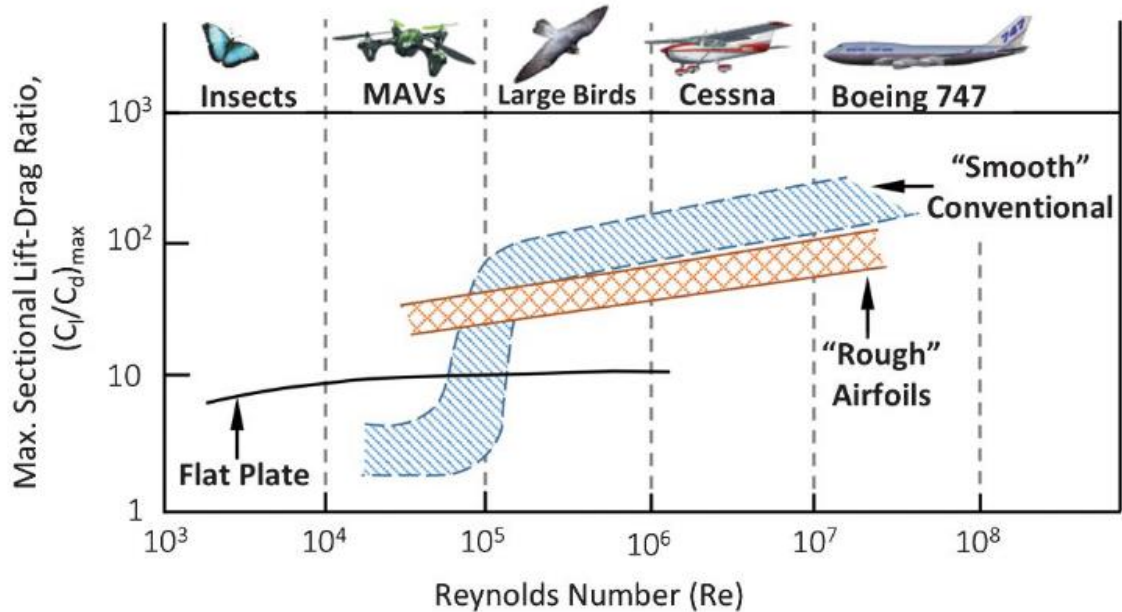


Figure 2.1 Effect of Reynolds number on airfoil maximum sectional lift-to-drag ratio
(Winslow et al., 2018)

Although earlier studies' experimental data are helpful for understanding trends in low Reynolds number aerodynamics, they are not without flaws. Previous research on Reynolds numbers below 10^5 has usually only included lift and drag data for a single Reynolds number for each airfoil (Michael S. Selig et al., 1995), which is insufficient to describe its performance throughout the range adequately. Furthermore, data sets with a score of less than 10^5 include uncertainties and inconsistencies. For example, drag measurements towards the E387 airfoil (9.1% t/c, 3.2% camber) at a Reynolds number of 6×10^4 varied by 28% – 68% between independent measurements taken at different facilities (M. Selig et al., 1995), whereas drag measurements at a